Effective quantum dimer model for trimerized kagomé antiferromagnet

M. E. Zhitomirsky
Commissariat à l'Energie Atomique, DSM/DRFMC/SPSMS, 38054 Grenoble, France
(Dated: February 2, 2008)

An effective spin-orbit Hamiltonian is derived for a spin-1/2 trimerized kagomé antiferromagnet in the second-order of perturbation theory in the ratio of two coupling constants. Low-energy singlet states of the obtained model are mapped to a quantum dimer model on a triangular lattice. The quantum dimer model is dominated by dimer resonances on a few shortest loops of the triangular lattice. Characteristic energy scale for the dimer model constitutes only a small fraction of the weaker exchange coupling constant.

PACS numbers: 75.10.Jm, 75.50.Ee

I. INTRODUCTION

Resonating valence bond (RVB) state[1] is nowadays a popular paradigm in condensed matter physics. Short-range RVB states are considered to be probable candidates for an elusive spin-liquid phase of magnetic insulators. The idea of short-range RVB states is quantitatively formulated by so called quantum dimer models (QDM).[2,3,4] In a QDM each dimer represents a singlet state (valence bond) between a pair of neighboring spins. The QD Hamiltonian is defined in the Hilbert space of close-packed dimer coverings of a lattice. The dimer states are assumed to be properly orthogonalized. Local dynamics of an RVB state is typically described on the smallest plaquettes ($\square$), which are squares for a square lattice or rhombi for a triangular lattice:

$$\hat{\mathcal{H}}_{\rm QD} = \sum_{\square} \Big[-t\big(|{=}\rangle\langle{\shortparallel}| + |{\shortparallel}\rangle\langle{=}|\big) + V\big(|{=}\rangle\langle{=}| + |{\shortparallel}\rangle\langle{\shortparallel}|\big) \Big]. \tag{1}$$

The first term is a dimer kinetic energy, which flips a pair of parallel dimers around an arbitrary plaquette; the second term is a potential energy between such pairs.

Rokhsar and Kivelson[3] have shown that a short-range RVB state given by a superposition of all dimer coverings of a square lattice is an exact eigenstate of the QD Hamiltonian for a special choice of the parameters $t = V$. On a bipartite square lattice, the RVB state at the Rokhsar-Kivelson (RK) point has long-range power low correlations and describes, consequently, a gapless spin-liquid state.[3,5] Small perturbations away from the RK point drive the system into one of the ordered crystalline dimer states. The QDM on a triangular lattice exhibits quite a different behavior at the RK point.[5,7] The short-range RVB state has exponentially decaying correlators and is fully gapped. It exists, therefore, in a finite range of parameters around the RK point and is stable with respect to weak perturbations to the QD Hamiltonian. Still, question whether such states or Hamiltonians can describe realistic quantum spin systems remains unsettled. In the present work we propose a realization of QDM on a triangular lattice for a nearest-neighbor Heisenberg spin model.

The most probable candidates for a singlet spin-liquid ground state are frustrated quantum antiferromagnets.[8] Numerical exact diagonalization studies of a spin-1/2 Heisenberg kagomé antiferromagnet have shown that this spin model has a nonmagnetic ground state with a large number of low-lying singlet excitations.[9,10] Accessible cluster sizes do not allow to draw a definite conclusion on the possible nature of the magnetically disordered (singlet) ground state.

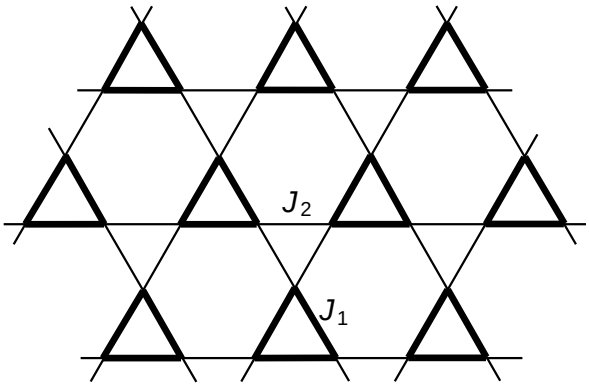

FIG. 1: Trimerized kagomé lattice with two exchange constants: J_1 in $\triangle$-triangles and J_2 in $\triangledown$-triangles.

One of a very few analytic approaches to such strongly-correlated spin systems is an expansion from small clusters. The main motif of a kagomé lattice is triangle. It is, therefore, natural to start from a trimerized kagomé lattice shown in Fig. 1. Such a strong-coupling approach has been pursued in relation to kagomé antiferromagnet in several theoretical works.[11,12,13,14] Recently, an experimental scheme to create a trimerized kagomé lattice has been suggested for ultracold atomic gases in optical traps.[15] This opens a way for an experimental probe of RVB physics in the corresponding spin model.

The Heisenberg model on a trimerized lattice

$$\hat{\mathcal{H}} = \sum_{\langle ij \rangle} J_{ij} \mathbf{S}_i \cdot \mathbf{S}_j \tag{2}$$

has two coupling constants: J_1 for a stronger interaction between spins in $\triangle$-triangles and J_2 for a weaker interaction inside $\triangledown$-triangles. An array of isolated $\triangle$-blocks is a

zeroth order Hamiltonian, which has a highly degenerate ground state. Interblock interaction lifts such a degeneracy. In section II we derive an effective Hamiltonian up to the second-order in a small parameter $J = J_2/J_1 \ll 1$. This Hamiltonian is mapped to a QDM in section III. The obtained results and their implication for the ground state properties of the trimerized kagomé model are discussed in section IV.

II. STRONG-COUPLING EXPANSION

A. First-order Hamiltonian

Let us in the beginning rederive the previous results on the effective first-order Hamiltonian[11,12,13] using somewhat different notations. Below we normalize all energies to J_1 such that $J_2 \to J$. In a strong-coupling expansion one starts with an isolated triangle described by

$$\begin{aligned}\hat{\mathcal{H}}_{\triangle} &= \mathbf{S}_1\cdot\mathbf{S}_2 + \mathbf{S}_2\cdot\mathbf{S}_3 + \mathbf{S}_3\cdot\mathbf{S}_1 \\ &= \frac{1}{2}\big(\mathbf{S}_1+\mathbf{S}_2+\mathbf{S}_3\big)^2 - \frac{3}{2}S(S+1)\ . \end{aligned} \quad (3)$$

The energy levels of $\hat{\mathcal{H}}_{\triangle}$ are determined by the total spin $S_{\rm tot}$. For on-site $S = 1/2$, which is always assumed below, the levels are two degenerate doublets with $S_{\rm tot} = 1/2$ and $E = -\frac{3}{4}$ and one quartet with $S_{\rm tot} = 3/2$ and $E = \frac{3}{4}$. The doublet states with $S^z_{\rm tot} = 1/2$ are

$$|d_\uparrow\rangle = \frac{1}{\sqrt{2}}\big(\uparrow\uparrow\downarrow - \uparrow\downarrow\uparrow\big),\quad |p_\uparrow\rangle = \frac{1}{\sqrt{6}}\big(2\downarrow\uparrow\uparrow - \uparrow\uparrow\downarrow - \uparrow\downarrow\uparrow\big), \quad (4)$$

where spin numbering in an individual triangle follows Fig. 2a. The former state $|d_\uparrow\rangle$ is a combination of the spin-up apex spin and a singlet bond between the two base spins and has odd parity under the permutation $\hat{P}_{23}$. The other state $|p_\uparrow\rangle$ is even under $\hat{P}_{23}$. The two members of a quartet with $S^z_{\rm tot} = +3$ and $+1$ are

$$|q_{+3}\rangle = |\uparrow\uparrow\uparrow\rangle\ ,\quad |q_{+1}\rangle = \frac{1}{\sqrt{3}}\big(\downarrow\uparrow\uparrow + \uparrow\downarrow\uparrow + \uparrow\uparrow\downarrow\big)\ . \quad (5)$$

All other states are obtained from (4) and (5) by applying $S^-_{\rm tot}$ operator.

The choice of the basis in the doublet subspace is not unique. The apex spin can be put into a singlet state either with its right or left neighbor. The two alternative basis states obtained by rotating $|d_\uparrow\rangle$ about a center of triangle counterclockwise on $2\pi/3$ and $4\pi/3$ are

$$|d'_\uparrow\rangle = \frac{1}{\sqrt{2}}\big(\downarrow\uparrow\uparrow - \uparrow\uparrow\downarrow\big)\ ,\quad |d''_\uparrow\rangle = \frac{1}{\sqrt{2}}\big(\uparrow\downarrow\uparrow - \downarrow\uparrow\uparrow\big) \quad (6)$$

with their orthogonal partners $|p'_\uparrow\rangle$ and $|p''_\uparrow\rangle$. Transformation from the old basis (4) to the new states is

$$\begin{aligned}&|d'_\alpha\rangle = -\frac{1}{2}|d_\alpha\rangle + \frac{\sqrt{3}}{2}|p_\alpha\rangle,\ |p'_\alpha\rangle = -\frac{\sqrt{3}}{2}|d_\alpha\rangle - \frac{1}{2}|p_\alpha\rangle, \\ &|d''_\alpha\rangle = -\frac{1}{2}|d_\alpha\rangle - \frac{\sqrt{3}}{2}|p_\alpha\rangle,\quad |p''_\alpha\rangle = \frac{\sqrt{3}}{2}|d_\alpha\rangle - \frac{1}{2}|p_\alpha\rangle, \end{aligned} \quad (7)$$

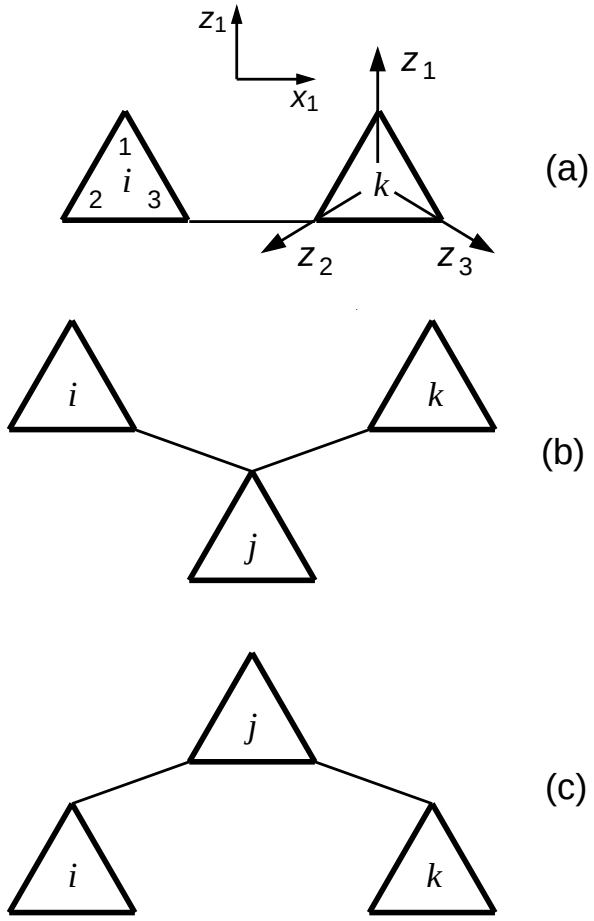

FIG. 2: Three different geometries of $\triangle$-blocks contributing to the second-order energy correction in the interblock coupling. The labeling of axes and sites inside triangles is shown in the upper panel (a).

where $\alpha = \uparrow, \downarrow$ or 1,2 is a spinor index. The main difference with the previous works[11,12] is that real basis states (4) or (7) are used instead of complex chiral states. This yields a more transparent form of the effective Hamiltonian and simplifies subsequent derivation of a QDM.

At this point we introduce two sets of the Pauli matrices: σ^i, which act between spin-up and spin-down states, and τ^i, which act in the orbital subspace (d, p) preserving the total spin. A convenient choice of orbital axes shown in Fig. 2a corresponds to

$$\tau^{z_1}|d_\alpha\rangle = |d_\alpha\rangle\ ,\quad \tau^{z_1}|p_\alpha\rangle = -|p_\alpha\rangle\ . \quad (8)$$

Then, the orbital operators projected onto the rotated axes

$$\tau^{z_2} = -\frac{1}{2}\tau^{z_1} - \frac{\sqrt{3}}{2}\tau^{x_1},\quad \tau^{z_3} = -\frac{1}{2}\tau^{z_1} + \frac{\sqrt{3}}{2}\tau^{x_1} \quad (9)$$

have the following eigenstates:

$$\begin{aligned}&\tau^{z_2}|d'_\alpha\rangle = |d'_\alpha\rangle\ ,\quad \tau^{z_2}|p'_\alpha\rangle = -|p'_\alpha\rangle\ , \\ &\tau^{z_3}|d''_\alpha\rangle = |d''_\alpha\rangle\ ,\quad \tau^{z_2}|p''_\alpha\rangle = -|p''_\alpha\rangle\ . \end{aligned} \quad (10)$$

In order to find the effect of interblock coupling in the first order of perturbation theory in $J = J_2/J_1$ one should neglect $S_{\rm tot} = 3/2$ states separated by a finite gap $\Delta E = \frac{3}{2}$ and calculate matrix elements of the on-site spin operators between the low-energy doublet states $|d_\alpha\rangle$ and $|p_\alpha\rangle$. This problem is greatly simplified once all symmetries are taken into account. Introducing operators $d^\dagger_\alpha|0\rangle = |d_\alpha\rangle$ and $p^\dagger_\alpha|0\rangle = |p_\alpha\rangle$, where $|0\rangle$ is a fictitious vacuum, the Hubbard-type representation of on-site spins is written as

$$\mathbf{S}_1 = \frac{1}{2}\, d^\dagger_\alpha \boldsymbol{\sigma}_{\alpha\beta} d_\beta - \frac{1}{6}\, p^\dagger_\alpha \boldsymbol{\sigma}_{\alpha\beta} p_\beta \ , \qquad (11)$$
$$\mathbf{S}_{2,3} = \frac{1}{3}\, p^\dagger_\alpha \boldsymbol{\sigma}_{\alpha\beta} p_\beta \pm \frac{1}{2\sqrt{3}} \left(p^\dagger_\alpha \boldsymbol{\sigma}_{\alpha\beta} d_\beta + \text{h. c.} \right) .$$

Spinor structure is a consequence of the spin-rotation symmetry, while permutation of the base spins $\hat{P}_{23}$ fixes the orbital part in (11). The above representation is further simplified once the total spin of a triangle $\mathbf{S} = \frac{1}{2}\boldsymbol{\sigma}$ is defined and the orbital operators τ^{z_k} are used. Then, the $n^{\rm th}$ spin ($n = 1$–3) of the $i^{\rm th}$ triangular block is represented by

$$\mathbf{S}_{ni} = \frac{1}{3}\, \mathbf{S}_i \left(1 + 2\tau_i^{z_n}\right), \qquad (12)$$

where $\hat{\mathbf{z}}_n$ goes from the center of a triangle in the direction of the corresponding spin, see Fig. 2a.

The effective first-order Hamiltonian in the interblock coupling is found by substituting Eq. (12) into the Hamiltonian (2):

$$\hat{\mathcal{H}}_1 = \frac{J}{9} \sum_{\langle ij \rangle} \mathbf{S}_i \cdot \mathbf{S}_j (1 + 2\tau_i^{z_n})(1 + 2\tau_j^{z_m}) \ , \qquad (13)$$

where a trivial constant term $-\frac{3}{4}N_\triangle$ is omitted for convenience. The derived spin-orbital Hamiltonian $\hat{\mathcal{H}}_1$ is defined on a triangular lattice, such that every site corresponds to one $\triangle$-block of the trimerized kagomé model and is attributed with spin and orbital operators. The bond orientation uniquely determines the orbital axes for two participating sites.

B. Second-order Hamiltonian

The second-order energy corrections for weakly-coupled spin triangles have been obtained by Raghu and co-workers.[13] These authors have mostly been interested in a one-dimensional model, therefore, their analysis misses several terms relevant for a two-dimensional array of triangles in the trimerized kagomé model. In order to calculate the second-order result in J_2 one needs to determine matrix elements of on-site spins between doublet (4) and quartet (5) states. Introducing symmetric third-rank spinor tensor $q_{\alpha\beta\gamma}$ such that $q_{111} = |q_{+3}\rangle$, $q_{112} = \frac{1}{\sqrt{3}}|q_{+1}\rangle$ $q_{122} = \frac{1}{\sqrt{3}}|q_{-1}\rangle$, and $q_{222} = |q_{-3}\rangle$, and utilizing spin-rotation symmetry we find by analogy with Eq. (11)

$$\mathbf{S}_1 = -\frac{i}{\sqrt{6}}\, q^\dagger_{\alpha\beta\gamma} \big(\boldsymbol{\sigma}\sigma^y\big)_{\beta\gamma} p_\alpha + \text{h. c.} \ , \qquad (14)$$
$$\mathbf{S}_{2,3} = \frac{i}{\sqrt{6}}\, q^\dagger_{\alpha\beta\gamma} \big(\boldsymbol{\sigma}\sigma^y\big)_{\beta\gamma} \Big(\pm \frac{\sqrt{3}}{2} d_\alpha + \frac{1}{2} p_\alpha \Big) + \text{h. c.}$$

The second-order energy correction in the interblock coupling is, generally, given by

$$\hat{\mathcal{H}}_2(G, G') = \sum_X \frac{\langle G|\hat{\mathcal{H}}|X\rangle\langle X|\hat{\mathcal{H}}|G'\rangle}{E_G - E_X} \ , \qquad (15)$$

where G and G' denote combinations of lowest doublet states on $\triangle$-blocks and X are excited states. The nonzero second-order terms appear if either (i) one J_2-bond acts twice in the numerator of Eq. (15) or (ii) two adjacent J_2-bond emerging from the same $\triangle$-block are used subsequently in the matrix elements $\langle G|\hat{\mathcal{H}}|X\rangle$ and $\langle X|\hat{\mathcal{H}}|G'\rangle$. This determines three different geometries for two- and three-block interaction terms shown in Fig. 2. In the first case of two-block interaction, Fig. 2a, either one or both triangular blocks have quartets in the intermediate states X. For the three block interactions (Fig. 2b,c), only a middle block has excited quartets in the intermediate states. Every pair of free (uncoupled) spins in a $\triangle$-block imposes an extra permutation symmetry on the second-order Hamiltonian $\hat{\mathcal{H}}_2(G, G')$. For example, the two-block cluster in Fig. 2a has extra $\hat{P}_{12}$ symmetry for the left i-block and $\hat{P}_{13}$ symmetry for the right k-block. Therefore, the orbital states, $|d''_\alpha\rangle$ or $|p''_\alpha\rangle$ for the left block and $|d'_\alpha\rangle$ or $|p'_\alpha\rangle$ for the right block, remain unchanged during the second-order perturbation process (15). In other words $\hat{\mathcal{H}}_{2a}$ commutes with $\tau_i^{z_3}$ and $\tau_k^{z_2}$. The conservation of orbital state is also fulfilled for all triangles in the three-block term in Fig. 2b and for the side triangles in Fig. 2c, whereas the middle block does change its orbital state during the second-order process. The above conservation laws significantly simplify summation over intermediate states in Eq. (15). The final results are

$$\hat{\mathcal{H}}_{2a} \ = \ -\frac{J^2}{54} \sum_{\langle ik \rangle} \Big[(3 + 4\,\mathbf{S}_i \cdot \mathbf{S}_k)(1 - \tau_i^{z_l}\tau_k^{z_m}) + (1 - \tau_i^{z_n})(1 - \tau_k^{z_m}) \Big] \qquad (16)$$

for the two-block interaction;

$$\hat{\mathcal{H}}_{2b} = -\frac{4J^2}{243} \sum_{\langle ijk \rangle} \mathbf{S}_i \cdot \mathbf{S}_k (1 + 2\tau_i^{z_l})(1 + 2\tau_k^{z_m})(1 - \tau_j^{z_n}) \qquad (17)$$

for the three-block interaction shown in Fig. 2b with corresponding labeling of blocks; and

$$\hat{\mathcal{H}}_{2c} \ = \ \frac{2J^2}{243} \sum_{\langle ijk \rangle} (1 + 2\tau_i^{z_n})(1 + 2\tau_k^{z_n}) \Big[\mathbf{S}_i \cdot \mathbf{S}_k (1 + 2\tau_j^{z_n}) + \sqrt{3}\, \tau_j^y\, \mathbf{S}_i \cdot (\mathbf{S}_j \times \mathbf{S}_k) \Big] \qquad (18)$$

for the three-block interaction in geometry of Fig. 2c. Polarization of orbital operators $\tau_i^{z_n}$ in the above equations is again found by simple inspection of the arrangement of corresponding blocks on a trimerized kagomé lattice. Three-block terms in $\hat{\mathcal{H}}_{2b}$ exist on $\bigtriangledown$-plaquettes of an effective triangular lattice with three different z-axes in Eq. (17). Three-body terms in $\hat{\mathcal{H}}_{2c}$ appear on $\bigtriangleup$-plaquettes of the triangular lattice with one polarization of τ^z operators in Eq. (18), which changes under permutation of (ijk).

The interactions $\hat{\mathcal{H}}_{2a}$ and $\hat{\mathcal{H}}_{2c}$ coincide up to a trivial change of notations with the previously derived terms for a one-dimensional array of triangles,[13] while the term $\hat{\mathcal{H}}_{2b}$ is a novel one. Note, that $\hat{\mathcal{H}}_{2c}$ contains a remarkable three-body spin-chiral interaction term. By deriving the effective spin-orbital Hamiltonians $\hat{\mathcal{H}}_1$ and $\hat{\mathcal{H}}_2$, we have substantially restricted the Hilbert space and simplified the original problem of finding the ground and the lowest energy states of the spin model (2). The remaining problem of solving $\hat{\mathcal{H}}_1 + \hat{\mathcal{H}}_2$ is still highly nontrivial. The spin-orbital Hamiltonian $\hat{\mathcal{H}}_1$ has been studied so far in the mean-field approach.[12] An effective Hamiltonian derived by the contractor renormalization group, which partially resembles $\hat{\mathcal{H}}_1 + \hat{\mathcal{H}}_2$, has also been analyzed in the mean-field approximation.[14] Below we discuss a mapping of the derived Hamiltonians (13) and (16)–(18) to an effective QDM. The obtained QD Hamiltonian is dominated by the kinetic energy for dimer tunneling. The mean-field approximation, which assumes a frozen pattern of dimers, is, therefore, a poor approximation in the present problem.

III. QUANTUM DIMER MODEL

A. General remarks

Search for the low-energy states of the first-order Hamiltonian (13) can be started by considering first a two-site problem (two adjacent $\bigtriangleup$-blocks of the original kagomé lattice).[12] This problem is solved exactly and its ground state corresponds to a spin singlet with the orbital degrees fully polarized along the bond: $\langle \tau_i^{z_n} \rangle = \langle \tau_j^{z_m} \rangle = 1$. The ground-state energy is $-\frac{3}{4}J$. A variational singlet ground state for the lattice problem (13) is constructed by splitting the whole lattice into a close-packed structure of dimers between nearest-neighbor sites, such that the dimer wave-function is given by the ground-state solution of the two-site problem. A remarkable feature of these variational states is that at the mean-field level with respect to orbital degrees of freedom the total energy is just a sum of energies of individual dimers and does not depend on a particular dimer covering of a triangular lattice.[12] Indeed, once $\langle \tau_i^{z_n} \rangle = 1$, then for the two other axes $\langle \tau_i^{z_m} \rangle = \langle \tau_i^{z_k} \rangle \equiv -\frac{1}{2}$. Therefore, the expectation value of any empty bond, *i.e.*, a bond without a dimer, identically vanishes over the variational wave-function:

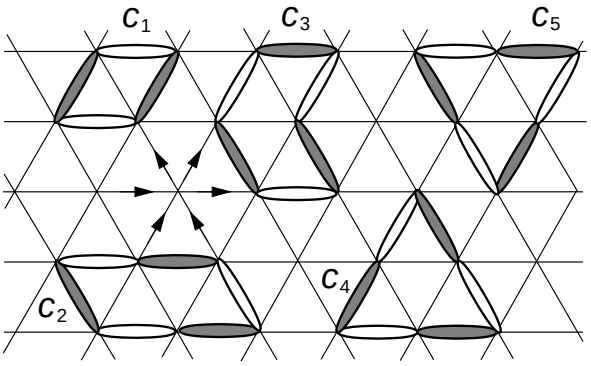

FIG. 3: Effective triangular lattice with five shortest loops. The arrow directions indicate the sign convention for singlet wave-functions on each bond

either one or both sites of the bond have $\langle 1 + 2\tau_i^{z_m} \rangle \equiv 0$.

The degenerate set of variational mean-field states has been identified with low energy states of spin-1/2 antiferromagnets on trimerized and isotropic kagomé lattices.[12,16] The number of low-lying singlets of the kagomé model scales, then, as 1.15^N in good agreement with the full exact diagonalization study.[10] The previous works leave, however, without answer question about validity of the mean-field approximation and further lifting of degeneracy by quantum fluctuations.

In order to beyond the mean-field approximation, one has to consider off-diagonal matrix elements of the Hamiltonian (13) between various dimer configurations as well as the corresponding overlap matrix. The general rule to compute the overlap matrix for models, where every dimer represents a singlet pair, is to construct transition or overlap graph by drawing two dimer configurations on the same lattice.[2] Every closed nonintersecting loop of dimers contributes $2/2^{l/2}$ to the overlap matrix, l being the length of the loop. The sign of the overlap matrix element depends on a sign convention for singlet wave-functions. We adopt the standard convention[2,5,6] such that the singlet bond wave-function is $[ab] = \frac{1}{\sqrt{2}}(\uparrow_a\downarrow_b - \downarrow_a\uparrow_b)$, where b is an upper site in the pair or is directly to the right from a, see Fig. 3.

Local dynamics of singlet bonds in trimerized kagomé model is determined by a few shortest loops on an effective triangular lattice, which include two- and three-dimer moves, see Fig. 3. Taking into account the orbital part of the wave-functions the overlaps of two dimer configurations on each loop are calculated as $c_1 = -1/2^4$, $c_2 = c_3 = -1/2^7$, $c_4 = -1/2^8$, and $c_5 = 1/2^5$. These overlap matrix elements are significantly smaller than for singlet bond configurations on the original triangular lattice. In the latter case the corresponding loops have $c_1 = 1/2$, $c_2 = c_3 = 1/2^2$, $c_4 = c_5 = -1/2^2$. The difference reflects the fact that loops on an effective triangular lattice correspond to significantly longer loops on the original trimerized kagomé lattice. For example, the shortest C_1 loop corresponds to a loop of length $l = 10$ on a kagomé lattice. Loops C_4 and C_5 are different for

the considered model because kagomé lattice has only a three-fold rotation axis in the center of every triangle. Significant difference of the overlap matrix elements explains why a QDM description is a poor approximation for a spin-1/2 Heisenberg antiferromagnet on a triangular lattice,[1] but may be a good one for the trimerized kagomé antiferromagnet. Below in this section we assume that the ground states of the first and second-order effective Hamiltonians are given variationally by close-packed dimer states and compute a new effective QD Hamiltonian. The above assumption is supported by numerical treatment of the trimerized kagomé antiferromagnet.[16]

Derivation of a QDM from a particular spin Hamiltonian has been formulated via calculation of the inverse square root of the overlap matrix.[3] We find that actual calculations become more transparent by operating with the wave-functions. The final result are, of course, equivalent in both approaches. Specifically, let us consider two linearly independent, normalized states $|\psi_1\rangle$ and $|\psi_2\rangle$, which have a small overlap $\langle\psi_1|\psi_2\rangle = \langle\psi_2|\psi_1\rangle = c$. Matrix elements of the Hamiltonian between the two states are assumed to be known $E_{11} = \langle\psi_1|\hat{H}|\psi_1\rangle$, $E_{21} = E_{12} = \langle\psi_1|\hat{H}|\psi_2\rangle$, and $E_{22} = \langle\psi_2|\hat{H}|\psi_2\rangle$. The aim is to compute matrix elements in a new properly orthogonalized basis $|\varphi_n\rangle$. Transformation to the new basis is given by a symmetric matrix:

$$|\varphi_1\rangle = \lambda\big(|\psi_1\rangle - \mu|\psi_2\rangle\big),\ |\varphi_2\rangle = \lambda\big(|\psi_2\rangle - \mu|\psi_1\rangle\big)\ . \quad (19)$$

Conditions $\langle\varphi_1|\varphi_2\rangle = 0$, $\langle\varphi_1|\varphi_1\rangle = \langle\varphi_2|\varphi_2\rangle = 1$ determine μ and λ. Assuming $E_{11} = E_{22}$, for simplicity, and calculating matrix elements of $\hat{\mathcal{H}}$ between the new states one finds

$$\tilde{E}_{11} = E_{11} + \frac{c}{1-c^2}\big(cE_{11} - E_{12}\big)\ ,$$
$$\tilde{E}_{12} = E_{12} + \frac{c}{1-c^2}\big(cE_{12} - E_{11}\big)\ . \quad (20)$$

In the following we shall subtract from the effective Hamiltonians $\hat{\mathcal{H}}_1$ and $\hat{\mathcal{H}}_1 + \hat{\mathcal{H}}_2$ the corresponding mean-field energies $E_{\rm MF}$, which are the same for all dimer coverings. Then, $E_{11} = E_{22} = 0$ and the matrix elements (20) are directly related to the parameters of a QDM:

$$t = -\tilde{E}_{12} \approx -E_{12}\ , \quad V = \tilde{E}_{11} \approx -cE_{12}\ , \quad (21)$$

where $|c| \ll 1$ is used.

B. First-order mapping

Let us apply the outlined procedure to the first-order Hamiltonian (13). The mean-field energy $E_{\rm MF} = -\frac{3}{4}JN_d$ of an arbitrary configuration of N_d dimers is always subtracted from Eq. (13). The wave-functions for two dimer states on the shortest loop C_1 shown in Fig. 3 are written explicitly as

$$|\psi_1\rangle = [12][43]|d_1 d_2' d_3' d_4\rangle,\ |\psi_2\rangle = [32][41]|d_1' d_2' d_3'' d_4''\rangle, \quad (22)$$

where sites are numbered counter-clockwise beginning with the lower right corner of the rhombus. The first part of $|\psi_{1,2}\rangle$ is given by a product of two spin singlet states, whereas the second part is an orbital wave-function represented as a product of states (4) or (7). Explicit calculation of the off-diagonal matrix element $E_{12} = \langle\psi_2|\hat{\mathcal{H}}_1|\psi_1\rangle$ yields

$$t_1 = -\frac{3}{2^6}J\ , \qquad V_1 = \frac{3}{2^{10}}J\ . \quad (23)$$

The largest kinetic energy term in the QD Hamiltonian (1) amounts to less than 5% of the weaker coupling constant. The ratio of the potential energy to the kinetic term constant is also very small $V/|t| = 1/16$. Note, that $t < 0$ from the above calculation. Remaining freedom in the choice of sign of tunneling matrix elements is discussed in the next section.

Since the potential energy V_1 is an order of magnitude smaller than the dimer hopping t_1, the next relevant interactions besides the kinetic energy of two-dimer moves around C_1 may be three-dimer resonances along longer loops C_2, C_3, C_4, and C_5. We find no tunneling for loops C_4 and C_5, *i.e.*, $V_{4,5} = t_{4,5} \equiv 0$. For loop C_5, vanishing of the off-diagonal matrix element can be understood by drawing two dimer configurations on a corresponding cluster of a kagomé lattice, which is a six-point star. Two dimer states around perimeter of such a star are exact degenerate eigenstates[17] and, hence, $t_5 \equiv 0$. In the former case, loop C_4, the $E_{12} = 0$ result is valid only in the first order in J, see the next subsection.

Coherent motion of three dimers along composite loops C_2 and C_3 is not described by Eqs. (20) and (21) because of resonances around small rhombi. Let the additional state with three parallel dimers on the parallelogram C_2 be denoted by $|\psi_1\rangle$ and the two dimer states on the perimeter of C_2 be $|\psi_2\rangle$ and $|\psi_3\rangle$, $\langle\psi_{2,3}|\psi_1\rangle = c$, while $\langle\psi_2|\psi_1\rangle = c'$. Then, the matrix elements $E_{12} = E_{13}$ describe short-loop resonances, while E_{23} corresponds to a tunneling along the composite loop. Generalizing transformation (19) to three states we finally obtain:

$$\tilde{E}_{11} \approx -cE_{12} - \big(c' - \frac{3}{4}c^2\big)E_{23}\ ,$$
$$\tilde{E}_{12} \approx E_{12}\ ,\quad \tilde{E}_{23} \approx E_{23} - cE_{12} \quad (24)$$

in the relevant case $|c'| \ll |c| \ll 1$. Tunneling of dimers along a longer loop E_{23} is renormalized by short-loop hopping. Using the above expressions to calculate resonance of singlet bonds on C_2 and C_3 one obtains that in both cases

$$t_2 = t_3 = -\tilde{E}_{23} = -\frac{15}{2^{10}}J\ . \quad (25)$$

The potential energy given by the second term in $\tilde{E}_{11}$ in (24) is again extremely small $V_2/|t_2| \approx 0.02$ and can be completely neglected.[18] Further extension of the above calculations to longer loops show that tunneling matrix elements of four-dimer moves are rather small $\sim 0.07t_1$ and should also be neglected.

C. Second-order mapping

Analysis starts again with calculation of the mean-field contribution from $\hat{\mathcal{H}}_2$ to the ground state energy (diagonal matrix elements) for an arbitrary dimer state. Every dimer has a finite energy contribution from $\hat{\mathcal{H}}_{2b}$: $\frac{1}{6}J^2$, while all nondimer bonds receive mean-field contributions from $\hat{\mathcal{H}}_{2a}$: $-\frac{1}{12}J^2$. The total mean-field energy does not, therefore, depend on a chosen dimer covering of a triangular lattice and is equal to

$$E_{\rm MF} = \Big(-\frac{3}{4} - \frac{3}{8}J - \frac{1}{8}J\Big)\frac{N}{3} \ , \tag{26}$$

where N is number of sites on a kagomé lattice. The mean-field energy (26) is subtracted in the following from $\hat{\mathcal{H}}_1 + \hat{\mathcal{H}}_2$, such that all diagonal matrix elements vanish.

The off-diagonal matrix element of $\hat{\mathcal{H}}_2$ for the shortest loop C_1 has nonzero contributions from $\hat{\mathcal{H}}_{2a}$: $-\frac{1}{64}J^2$, and from $\hat{\mathcal{H}}_{2c}$: $-\frac{1}{48}J^2$. Combining them with the first-order result Eq. (23) we obtain

$$t_1 = -E_{12} = -\frac{3}{2^6}J\Big(1 - \frac{7}{9}J\Big) \ . \tag{27}$$

Similar calculation for the loops C_2 and C_3 yields

$$E_{23} = \frac{3}{2^8}J\Big(1 + \frac{1}{9}J\Big) \ . \tag{28}$$

Taking into account Eq. (20) the tunneling matrix element between orthogonal dimer states along the loop C_2 (C_3) becomes

$$t_2 = t_3 = -\tilde{E}_{23} = -\frac{15}{2^{10}}J\Big(1 - \frac{1}{15}J\Big) \ . \tag{29}$$

Loop C_4 also acquires a finite tunneling rate between the two dimer states in the second-order. The corresponding matrix element is, however, small $E_{12} \approx 0.003J^2$.

IV. DISCUSSION

Signs of the tunneling matrix elements calculated in the previous section have certain arbitrariness.[3,5] The negative sign of the resonance matrix element for the shortest loop C_1 can be changed to positive by a gauge transformation. For this, real singlet wave-functions have to be multiplied by complex factors $i^{n_r+n_{l,e}-n_{l,o}}$, where for a given dimer configuration n_r counts the number of dimers on links pointing upwards and right, $n_{l,e}$ ($n_{l,o}$) counts the number of dimers on links pointing upwards and left from sites with even (odd) vertical coordinates. Dimers on strictly horizontal bonds do not contribute to the phase factor. By this operation resonance moves along every C_1 loop pick up an extra (-1) factor, changing $t_1 \to -t_1$. At the same time, amplitudes of dimer tunneling along C_2 and C_3 loops do not change sign by the above gauge transformation: $t_{2,3} \to t_{2,3}$. An effective QD Hamiltonian for the trimerized kagomé antiferromagnet is, therefore, dominated by the kinetic energy terms for resonance moves between orthogonal dimer configurations $|\varphi_{c_n}\rangle$ and $|\varphi'_{c_n}\rangle$ for every loop C_n of three different types $n = 1$–3 on an effective triangular lattice:

$$\hat{\mathcal{H}}_{\rm QD} = \sum_{l_n} -t_n |\varphi_{c_n}\rangle\langle\varphi'_{c_n}| \ , \tag{30}$$

$$t_1 = \frac{3}{64}J\Big(1 - \frac{7}{9}J\Big), \quad t_2 = t_3 = -\frac{15}{1024}J\Big(1 - \frac{1}{15}J\Big).$$

Amplitudes for three-dimer tunneling processes have no significant smallness compared to the strongest resonance move: $t_{2,3}/t_1 \approx -0.31$ for $J \ll 1$. The kinetic coefficients t_n are differently renormalized by the second-order processes such that importance of three-dimer moves is further increased towards the isotropic limit: $t_{2,3}/t_1 \approx -0.5$ for $J = 0.5$ and $t_{2,3}/t_1 \approx -1$ as $J \to 1$.

The QDM (30) with only two-dimer resonances has been studied via mapping to a frustrated Ising model in transverse field.[5,6] The ground state of this dimer model is believed to be a crystalline $\sqrt{12}\times\sqrt{12}$ state, which consists of locally resonating dimer pairs and breaks translational symmetry of the lattice. Such a state should have a fully gapped excitation spectrum. Properties of the QDM (30) with several competing dimer resonances have not been studied so far. Dimer resonances along longer loops, though not very small, frustrate each other. The ground state of the realistic model (30) should not be, therefore, very far from the idealized model with t_1 terms only. In particular, we expect that the ground state breaks certain lattice symmetries. The excitation spectrum is also expected to be gapped unless a fine tuning of t_n drives the system towards an Ising-type transition point between two crystalline states.

In conclusion, the presented derivation of the QDM for a realistic Heisenberg spin model on trimerized kagomé lattice illustrates a generation of small energy scales in frustrated quantum magnets. The dimer resonance matrix elements in (30) are given by small fractions of a weaker exchange constant, *e.g.*, $t_1 \approx 0.047J$. In a wide temperature interval $t_1 \ll T \ll J$ the quantum spin systems is described by an RVB liquid of singlet pairs. At very low temperatures $T < t_1$ a valence bond crystal probably replaces an RVB state. The gap between the ground state and the first excited singlet levels is a fraction of t_1. It is extremely difficult to resolve such a tiny energy scale in the exact numerical diagonalization of small clusters. Similarly, the low-temperature regime $T \lesssim t_1$ might be beyond experimental reach for possible realizations of the spin-1/2 trimerized kagomé antiferromagnet. The dimer crystallization at $T = 0$ is driven by local resonances. Therefore, variational mean-field type approaches[12,14] are not capable to describe the precise nature of the corresponding ground states.

Acknowledgments

I thank to D. A. Ivanov and G. Jackeli for valuable discussions. The hospitality of the Condensed Matter Theory Institute of Brookhaven National Laboratory during the course of present work is gratefully acknowledged.

[1] P. Fazekas and P. W. Anderson, Philos. Mag. **30**, 423 (1974); P. W. Anderson, Science **235**, 1196 (1987).
[2] B. Sutherland, Phys. Rev. B **37**, R3786 (1988).
[3] D. S. Rokhsar and S. A. Kivelson, Phys. Rev. Lett. **61**, 2376 (1988).
[4] R. Moessner, S. L. Sondhi, and P. Chandra, Phys. Rev. Lett. **84**, 4457 (2000).
[5] R. Moessner and S. L. Sondhi, Phys. Rev. Lett. **86**, 1881 (2001).
[6] R. Moessner and S. L. Sondhi, Prog. Theor. Phys. Suppl. **145**, 37 (2002).
[7] A. Ioselevich, D. A. Ivanov, and M. V. Feigelman, Phys. Rev. B **66**, 174405 (2002).
[8] A. Auerbach, *Interacting Electrons and Quantum Magnetism* (Springer, New York, 1994).
[9] P. Lecheminant, B. Bernu, C. Lhuillier, L. Pierre, and P. Sindzingre, Phys. Rev. B **56**, 2521 (1997).
[10] C. Waldtmann, H.-U. Everts, B. Bernu, C. Lhuillier, P. Sindzingre, P. Lecheminant, and L. Pierre, Eur. Phys. J. B **2**, 501 (1998).
[11] V. Subrahmanyam, Phys. Rev. B **52**, 1133 (1995).
[12] F. Mila, Phys. Rev. Lett. **81**, 2356 (1998).
[13] C. Raghu, I. Rudra, S. Ramasesha, and D. Sen, Phys. Rev. B **62**, 9484 (2000).
[14] R. Budnik and A. Auerbach, Phys. Rev. Lett. **93**, 187205 (2004).
[15] L. Santos, M. A. Baranov, J. I. Cirac, H.-U. Everts, H. Fehrmann, and M. Lewenstein, Phys. Rev. Lett. **93**, 030601 (2004).
[16] M. Mambrini and F. Mila, Eur. Phys. J. B **17**, 651 (2000).
[17] A. V. Syromyatnikov and S. V. Maleyev, Phys. Rev. B **66**, 132408 (2002).
[18] similar results have recently been obtianed by F. Mila et al., private communication (2004).